NASA TT F-9514

NASA TT F-9514

DATA PROCESSING SYSTEMS IN SPACE BIOLOGY

R. M. Bayevskiy, A. D. Voskresenskiy, O. G. Gazenko,
A. D. Yegorov, N. A. Chekhonadskiy and V. I. Yazdovskiy

Translation of "Avtomaticheskiy kontrol' i metody
elektricheskikh izmereniy",
Trudy IV konferentsii, Tom II, 1962 g., pp. 100-105.
Redaktsionno-izdatel'skiy Otdel Sibirskogo Otdeleniya AN SSSR,
Novosibirsk, 1964

N65-29740
(ACCESSION NUMBER)
9
(PAGES)
(NASA CR OR TMX OR AD NUMBER)
(THRU)
1
(CODE)
04
(CATEGORY)

FACILITY FORM 602

GPO PRICE $

CFSTI PRICE(S) $

Hard copy (HC) 1.00

Microfiche (MF) .50

ff 653 July 65

NATIONAL AERONAUTICS AND SPACE ADMINISTRATION
WASHINGTON JUNE 1965

PROTECTION FROM PRIMARY COSMIC RADIATION AND PROTONS OF THE EARTH'S INNER RADIATION BELT *174

V.Ye.Dudkin, Ye.Ye.Kovalev, L.N.Smirennyy,
and M.A.Sychkov

29741

Data on the proton and electron concentration in the Earth's inner radiation belt, collected by the Agena and Explorer satellites, are used for establishing the proton spectrum of the belt. The electron flux at the center of the belt is given as 10^5 protons/cm^2·sec. A mean proton spectrum is used for calculating the required shielding of space capsules and astronauts exposed in space. Mean tissue doses for astronauts, as a criterion for radiation hazard, are calculated and tabulated for several arbitrary orbits. Safe altitudes of orbits and orbital inclination angles are given, taking secondary radiation in the shielding and in the astronaut's body by the primary cosmic radiation into consideration.

Author

PRIMARY COSMIC RADIATION

Primary cosmic radiation (PCR) consists mainly of protons, α-particles and heavier nuclei. Table 1 gives its composition, according to other papers (Bibl.1, 2). This composition covers the energy range up to 10^4 Mev/nucleon.

TABLE 1

COMPOSITION OF PRIMARY COSMIC RADIATION

PCR COMPONENT	Z	$\bar{A}$	PORTION,%
P	1	1	85.2
α	2	4	13.2
L (Li, Be, B)	3–5	10	0.2
M (C, O, N, F)	6–9	14	1.0
H	10	31	0.3
vH	20	51	0.1

The differential spectrum for all PCR components of energies above 1 Bev/nucleon is of the form

$$n(E)\,dE = CE^{-\gamma}dE,$$

* Numbers in the margin indicate pagination in the original foreign test.

where E is the total energy of a particle; γ is the spectral exponent, whose value (Bibl.1, 3-5) is 2.0 - 2.5. Depending on the extent of solar activity, the integral flux of PCR corresponds to 1.8 - 4.0 particles/cm^2·sec (Bibl.6-10).

The time variations of the PCR flux in space do not exceed a few percent. The angular distribution of this flux is customarily considered isotropic. The absorbed dose of PCR has been calculated by the technique given elsewhere /175 (Bibl.11). We have assumed the PCR composition given in Table 1, and have taken the spectral exponent γ as 2.4 for all PCR components. The differential spectrum of the PCR for the energy range below 1 Bev/nucleon was chosen on the basis of the considerations by Ginzburg (Bibl.1). Table 2 gives the results of calculations for a flux of 2.3 particles/cm^2·sec. Clearly, a considerable

TABLE 2

TISSUE DOSE FOR VARIOUS PCR COMPONENTS
(WITHOUT SHIELDING)

Characterization of Dose	Components					PCR
	P	α	M	H	vH	
Absorbed dose						
*mrad/day	6.2	3.7	3.4	5.0	4.1	22.4
*mrem/day	6.2	3.7	11.1	34.0	73	128
Contribution to dose, %						
Physical	27.7	16.5	15.2	22.3	18.3	100
Biological	4.9	2.9	8.7	26.6	56.9	100

Note. The relative biological effectiveness (RBE) has been calculated from the linear losses of energy, using the data of other papers (Bibl.12, 13).

part of the PCR dose is due to heavy nuclei. According to preliminary calculations, the contribution of nuclei of the L group to the dose is a few tenths of a percent so that we have neglected it here. If shielding is used, the contribution of the heavy elements to the dose decreases with increasing thickness of the shielding.

Figure 1 shows the distribution in depth of the dose absorbed in the body. Since the PCR is very hard, the intensity decreases only insignificantly from the surface toward the center. For shielding up to 10 gm/cm^2 in thickness, the dose absorbed in the body increases from the surface toward the center (see Fig.1), since the high-energy PCR particles are slowed in the body, with

* rad = absorbed dose of radiation; rem = roentgen equivalent, man.

a consequent increase in their ionization losses $\left(\frac{dE}{dx}\right)$. On further increase in the thickness of the shielding, the low-energy PCR particles begin to be

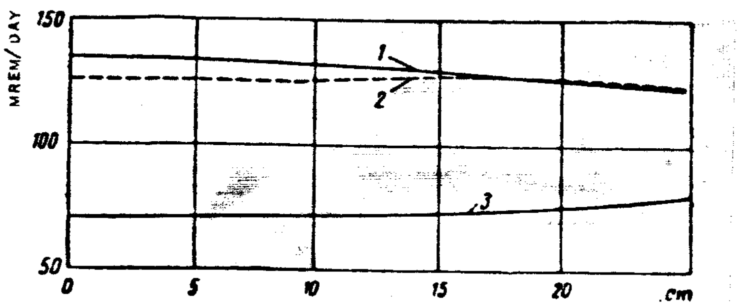

Fig.1 Distribution in Depth of PCR Dose through Light-Material Shielding of Varying Thickness:
1. No shielding; 2. thickness of shielding 10 gm/cm^2;
3. thickness of shielding 70 gm/cm^2

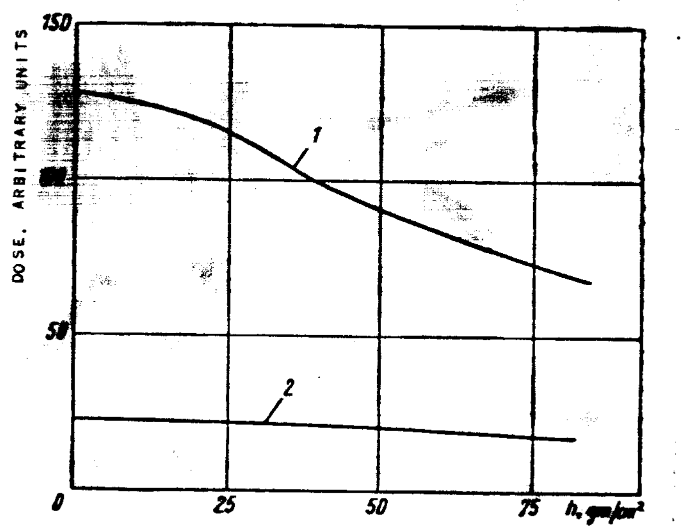

Fig.2 Relation of PCR dose to Thickness of Light-Material Shielding:
1. Dose in mrem/day; 2. dose in mrad/day

absorbed by the body. For this reason, the absorbed dose then decreases from the surface toward the center (Fig.2). On prolonged space flights, the PCR are a persistent component of the radiation. The maximum dose absorbed in the body must therefore be used as a criterion for radiation safety. However, as will be seen from Fig.1, the decline in the dose from the skin toward the /176 center of the body does not exceed about 10%. Thus, the radiation hazard due to PCR on space flights can be estimated from the mean tissue dose.

The total radiation effect of PCR without shielding was found to be 22.4 mrad/day or 128 mrem/day. With increasing thickness of the shielding, the PCR dose remains practically constant up to shielding thicknesses of 10 - 15 gm/cm^2 (see Fig.2). At very great thickness (being of the order of 70 - 100 gm/cm^2), the dose decreases by a factor of 1.5 - 2. For a rough /177 estimate of the contribution to the dose by secondary radiation formed in the shielding and in the astronaut's body under the action of the PCR, we used data on the altitude variation of the ionization produced by PCR in the atmosphere. This estimate showed the contribution of the secondary radiation to be 50-100%. Allowing for this, the PCR dose in interplanetary space might reach as much as 190 - 250 mrem/day.

The PCR dose near the Earth is considerably lower, owing to the shielding action of the Earth itself and of its magnetic field. Table 3 gives the calculated mean tissue or depth doses of PCR in the space surrounding the Earth.

TABLE 3

MEAN TISSUE DOSE OF PCR IN THE EXOSPHERE FOR SHIELDING OF THICKNESS 0 - 2gm/cm^2, IN mrem PER DAY OF FLIGHT*

ANGLE OF INCLINATION OF ORBITAL PLANE, IN DEGREES	ALTITUDE ABOVE EARTH'S SURFACE, km			
	200—600	100—1500	2500—3500	7500
0	5.0 (1.2)	5.5 (1.4)	15.2 (12.0)	59.6 (14.5)
45	12.7 (3.1)	20.8 (5.1)	38.5 (30.3)	73.7 (18.0)
65	22.8 (5.6)	33.3 (8.1)	51.0 (40.1)	77.9 (19.0)
90	27.3 (6.7)	37.4 (9.1)	54.1 (42.6)	78.7 (19.3)

* Dose in millirads after 24 hrs of flight is shown in parentheses.

Thus, the PCR dose near the Earth is only 1/20 as great as it is in interplanetary space. For an orbit at an altitude of 200 - 600 km with a 65^{o} inclination, the surface or skin dose, with shielding of 2 gm/cm^2, is about 8 - 11 mrad/day (including secondary radiation). The results of direct measurements on the 2nd, 4th and 5th spaceships (Bibl.14) and on the Gagarin and Titov flights (Bibl.15) are in agreement with this figure. The estimated doses given here show that for long space flights it will be necessary to take account of the radiation hazard from PCR, and of the fact that the biological effect of high-energy heavy nuclei has not yet been studied and may have its own peculiar features. On brief space flights, there is no danger whatever to the astronaut from the primary cosmic radiation.

THE EARTH'S INNER RADIATION BELT

The inner radiation belt is localized within the region bounded by the magnetic lines of force intersecting the Earth's surface at the geomagnetic latitude 45°. In the Western Hemisphere, this region begins at an altitude /178 of 500 - 600 km and in the Eastern Hemisphere, at an altitude of about 1500 km, extending outward to 5000 - 10,000 km into space. The maximum radiation intensity is observed at about 3600 km above the Earth's surface.

We selected the spatial distribution of the intensity of the protons of the inner radiation belt (Fig.3) on the basis of measurements made during the flight of the "Explorer VI" (Bibl.16, 17) and of theoretical calculations

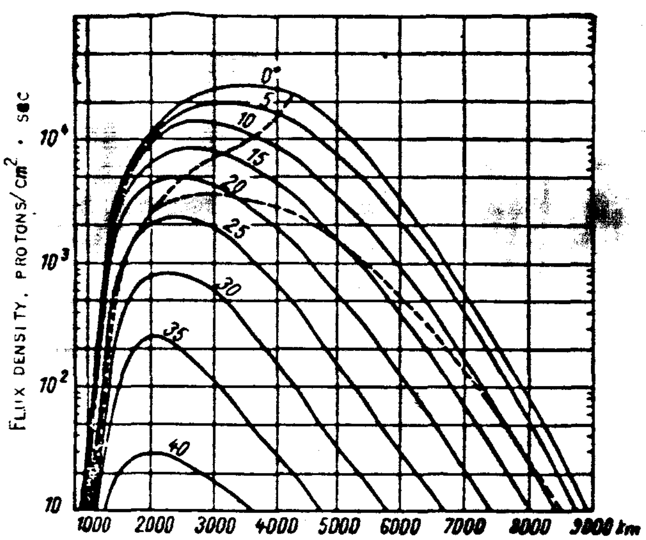

Fig.3 Relation between Omnidirectional Integral Proton Flux (E_p > 30 Mev) of the Inner Radiation Belt, Distance from the Earth's Surface, and Geomagnetic Latitude. The broken curves show zones of shadow and penumbra (forbidden zone for protons of solar origin or where they lack stable orbits)

taking the neutron albedo hypothesis into consideration (Bibl.18). The deformation of the belt due to magnetic anomalies was not taken into account. This picture of the spatial distribution of the inner belt is, of course, only approximate and will require correction as new experimental data are obtained. Thus, measurements on the interplanetary station "Mars-1" have shown that the zone of high intensity is farther from the Earth than was previously thought (Bibl.33).

The experimental data available today indicate the existence of a proton component and an electron component in the Earth's inner radiation belt. The experimental values of the fluxes at the center of the belt (Bibl.19) are as follows:

Protons: omnidirectional intensity /179

$$J_0(>40 \text{ Mev}) = 2 \times 10^4 \text{ protons/cm}^2 \cdot \text{sec}$$

(with accuracy to a factor of 2).

Electrons: maximum of unidirectional intensity

$$N(> 20 \text{ Kev}) = 2 \times 10^9 \text{ electrons/cm}^2 \cdot \text{sec}$$

(with accuracy to a factor of 10);

$$N(> 600 \text{ Kev}) \approx 1 \times 10^7 \text{ electrons/cm}^2 \cdot \text{sec}$$

(with an accuracy to a factor of 2).

According to other data recently obtained on the satellite "Agena", the electron flux at the center of the belt is 10^5 protons/cm^2·sec. Numerous measurements of the spectra of protons of the inner belt (Bibl.20 - 26) using nuclear emulsions and counters, have shown the spectrum to be of the form:

$$N(E)dE = N_0 E^{-n} dE,$$

where the exponent n, according to various data, has values from 1.4 (Bibl.24) to 1.8 (Bibl.20), depending on the region of the proton spectrum to which the measurements relate. The exponent n decreases with decreasing proton energy. The character of the spectrum also depends somewhat on the geomagnetic latitude of the test point, this relationship being particularly noticeable in the range of low proton energies (below 30 Mev). Thus, measurements made on 19 September 1960 (six days after a solar flare) showed considerably greater steepness ($n \approx 4.5$) of the low-energy region of the proton spectrum at high latitudes, and an appreciable increase in intensity (Bibl.16). Since these measurements were preceded by a solar flare, a low-energy anomalous component due to protons of solar origin was postulated.

In the energy range above 30 Mev, as shown by the "Explorer VI" measurements (Bibl.23), the proton spectrum is almost independent of the coordinates of the test point (the measurements were made in the latitude interval from -25.3 to -31.8° at a mean altitude of 2225 km above the Earth's surface). In this case the exponent was found to be 1.65.

Calculations of the proton spectra of the Earth's inner belt, based on the neutron-albedo hypothesis (Bibl.18, 21, 27) are in good agreement with the experimental spectrum in the energy region above 80 Mev. Agreement is poorer in the region of lower energies, owing to the indeterminacy of the neutron-albedo spectrum in this energy region.

On the basis of present experimental and theoretical data we selected the proton spectrum of the Earth's inner radiation belt for subsequent use in /180 calculating the required shielding. Figure 4 shows this spectrum. The proton spectra used heretofore for such calculations (Bibl.28, 29) differ substantially from the spectrum of Fig.4.

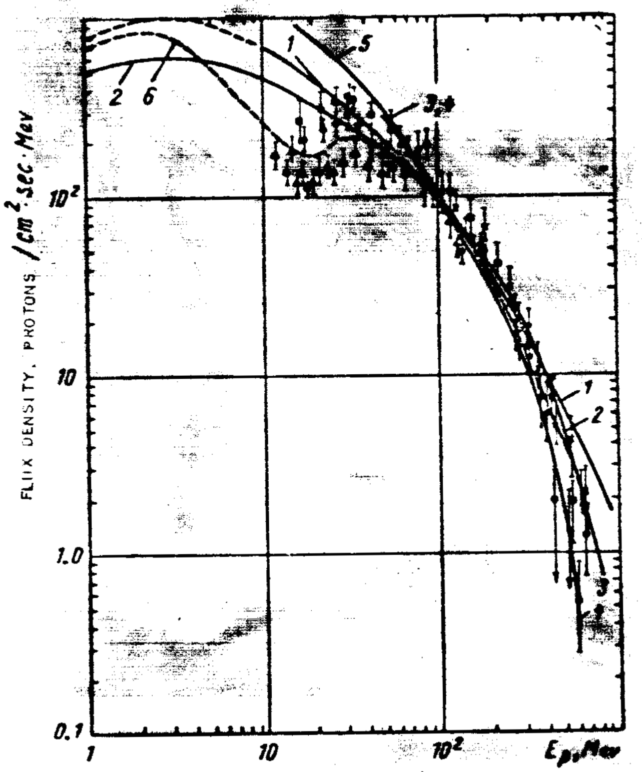

Fig.4 Proton Spectra of the Inner Radiation Belt (Standardized to 100 Mev);
1. Calculated spectrum (Bibl.21); 2. spectrum used in other papers (Bibl.27, 28); 3. calculated spectrum (limit energy E = 1000 Mev) (Bibl.18); 4. spectrum according to Nangle's data (Bibl.16); 6. mean spectrum used in our calculations; × – (Bibl.21); ◻ – (Bibl.20); o – (Bibl.22); ▲ – (Bibl.25); ● – (Bibl.26).

The shielding from the protons of the Earth's inner belt was calculated with the method given elsewhere (Bibl.11) as basis. The results are valid for a proton flux of 2×10^4 protons/cm^2·sec. We assumed the spaceship capsule to be spherical and made of aluminum (Bibl.31). The angular distribution of the protons incident on the shielding was assumed to be isotropic.

Figure 5 shows the relation between the mean tissue dose of protons of the Earth's inner belt and the thickness of aluminum shielding. For comparison the graph also gives similar relations for a local dose and a surface dose. It may be concluded from an analysis of these data that the estimate of a dose from the energy transferred to 1 gm of tissue (local dose) is considerably exaggerated: at small shielding thickness, the mean tissue dose is only 3–5 times /182

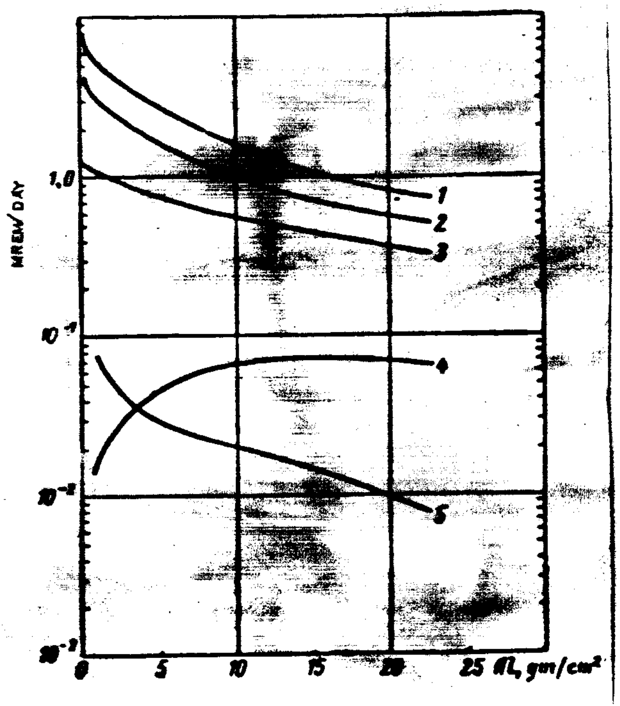

Fig.5 Relation between Dose of Primary and Secondary Radiation and Thickness of Shielding. The secondary radiation was estimated from Beck's data (Bibl.31)
1. local dose; 2. skin dose; 3. mean tissue dose; 4. secondary neutrons; 5. secondary protons.

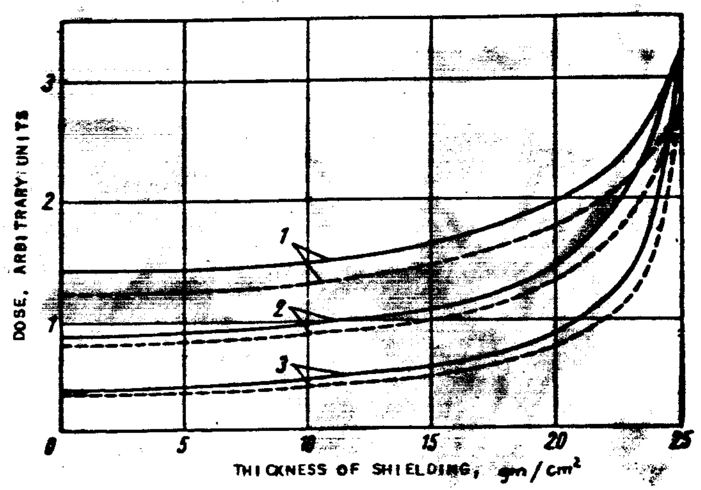

Fig.6 Depth Doses due to Protons of Inner Radiation Belt, for Shielding of Various Thicknesses (in Terms of Skin Dose)
1. Shielding thickness 20 gm/cm^{2}Al; 2. shielding thickness 10 gm/cm^2 Al; 3. shielding thickness 1 gm/cm^2 Al;
——— dose in rems; - - - dose in rads.

TABLE 4

MEAN TISSUE DOSES OF RADIATION FOR AN ASTRONAUT IN THE EXOSPHERE, mrem/day

ALTITUDE ABOVE EARTH'S SURFACE IN km	ANGLE OF INCLINATION OF ORBITAL PLANE AND THICKNESS OF SHIELDING, gm/cm²											
	0°			45°			65°			90°		
	1	10	20	1	10	20	1	10	20	1.	10	20
250	0.5	0.25	0.16	0.5	0.25	0.16	0.5	0.25	0.16	0.5	0.25	0.16
500	1.2	0.6	0.4	1.2	0.6	0.4	1.2	0.6	0.4	1.2	0.6	0.4
1000	150	77	50	52	27	18	41	[illegible]	14	38	19	13
2500—3500	$82\cdot10^3$	$42\cdot10^3$	$25\cdot10^3$	$20\cdot10^3$	$10\cdot10^3$	$6.6\cdot10^3$	[illegible]	$7.6\cdot10^3$	$5.0\cdot10^3$	$12.2\cdot10^3$	$6.3\cdot10^3$	$4.1\cdot10^3$
7500	190	97	63	38	20	13	[illegible]	15	10	28	14	9

smaller than the local dose. Here, the drop between the maximum (surface) dose and the mean tissue dose at a shielding thickness over 1 gm/cm^2, where the low-energy anomalous component has practically no effect, is not more than by about a factor of 3.

Thus, the character of the distribution in depth of the absorbed dose of inner-belt protons in the body is such (Fig.6) that the use of the mean tissue dose as a criterion for radiation hazard can be considered justified.

The results of the calculations shown in Fig.5 and the pattern of spatial distribution (see Fig.3) were used as the basis for calculating the mean tissue doses of radiation for an astronaut, for several arbitrarily selected circular orbits (Table 4).

Thus flights on circular orbits at an altitude of less than 1000 km or more than 7500 km above the Earth's surface, at an angle of orbital inclination over 45^o, will lead to irradiation of the astronaut with doses not exceeding 0.05 rem/day. With decreasing angle of inclination of the orbital plane, these doses may, under the above conditions, reach 0.15 - 0.20 rem/day.

Flights near the intensity maximum of the inner belt would involve irradiation of the astronaut with doses of 4 to 30 rem/day (depending on the angle of inclination θ, for a shielding thickness of the order of 20 gm/cm^2). It follows that a considerable thickness of the protective skin of the spaceship is required for prolonged flights. A brief crossing of the inner belt (5 - 15 min) under the most un- /183 favorable conditions (angle of inclination $\theta = 0^o$, thickness of shielding 1 gm/cm^2) can be considered entirely safe, since the radiation dose would not exceed 1 rem.

These data will have to be supplemented by estimates of the contribution to the dose made by the secondary radiation arising in the shielding and in the astronaut's body. The absorbed dose of secondary particles formed in shieldings up to 20 gm/cm^2 thickness is about 5 - 10% of the total dose (Bibl.28, 30-32). The dose increase caused by secondary particles formed by the protons in the astronaut's body has been estimated by us on the basis of experimental data obtained with phantoms on a proton beam in the OIYaI synchrocyclotron. This contribution amounts to about 20%. Thus the absorbed dose must be increased by about 30% on account of the secondary particles formed by the protons in the shielding and in the astronaut's body. However, we wish to emphasize the merely approximate character of these estimates and the need for further experimental data.

BIBLIOGRAPHY

1. Ginzburg, V.L.: Uspekhi fiz. nauk, Vol.74, No.3, 1961.
2. Madey, R.: Preprint A.A.S., No.15, 1962.
3. Syrovatskiy, S.I.: Zhurn. eksper. i teor. fiz., Vol.40, No.6, p.1788, 1961.
4. McDonald, F.D.: Phys. Rev., Vol.109, p.1367, 1958.
5. Webber, W.R.: Nuovo cimento, Vol.8, p.532, 1958.
6. Vernov, S.N. et al: Dokl. AN SSSR, Vol.125, p.304, 1959.
7. Van Allen, J.A. and Frank, L.A.: Nature, Vol.183, p.430, 1959.
8. Vernov, S.N. and Chudakov, A.Ye.: Uspekhi fiz. nauk, Vol.70, p.585, 1960.
9. Langham, W.H.: Aerospace Med., Vol.30, p.410, 1959.
10. Kurnosova, L.V. et al: Iskusstv. sput. Zemli., No.5, p.30, 1960.
11. Dudkin, V.Ye. et al: Principal Methodological Questions in Calculating Shielding Against High-Energy Protons (Osnovnyye metodicheskiye voprosy rascheta zashchity ot protonov bol'shikh energiy). This Collection, p.159.
12. - NBS, Handbook, 59.
13. Snyder, W.S. and Neufeld, J.: Radiation Res., Vol.6, No.1, p.67, 1957.
14. Keirim-Markus, I.B., Kovalev, Ye.Ye., and Uspenskiy, L.N.: Iskusst. sput. Zemli., No.12, p.47, 1962.
15. Keirim-Markus, I.B. et al: Ibid. No.15, p.102, 1963.
16. Nangle, J.E. and Kniffen, D.A.: Phys. Rev. Lett., Vol.7, pp.3-6, 1961.
17. McIlwain, C.E.: J.Geophys. Res., Vol.66, p.3681, 1961.
18. Lenchek, A.M. and Singer, S.F.: J.Geophys. Res., Vol.67, No.4, p.1263, 1962.
19. Van Allen, J.A.: J.Geophys. Res., Vol.63, p.1683, 1959.
20. Freden, S.C. and White, R.S.: Phys. Rev. Lett., Vol.3, No.9, 1959.
21. Freden, S.C. and White, R.S.: J.Geophys. Res., Vol.65, No.5, p.1377, 1960.
22. Armstrong, A.H. et al: J. Geophys. Res., Vol.66, No.2, p.351, 1961.
23. Hoffman, R.A., Arnoldy, R.L., and Winckler, J.R.: J. Geophys. Res., Vol.67, No.1, p.1, 1962.
24. Holly, F.E. et al: J. Geophys. Res., Vol.66, p.1627, 1961.
25. Armstrong, A.H. and Heckman, H.H.: Geophys. Res., Vol.67, No.4, p.1255, 1962.
26. Freden, B.C. and White, R.S.: J.Geophys. Res., Vol.67, No.1, p.25, 1962.
27. Hess, W.H.: Phys. Rev. Lett., Vol.3, p.11, 1959.

28. Day, D.L. and Noyes, J.C.: J.Astron. Sci., Vol.II, No.3, p.64, 1960.
29. Shaefer, H.J.: Aerospace Med., Vol.31, No.10, p.807, 1960.
30. Ivanov, V.I., Keirim-Markus, I.B., and Kovalev, Ye.Ye.: Iskusst. sput. Zemli, No.12, p.35, 1962.
31. Beck, A.J. and Divita, E.L.: ARS Journal, Vol.11, p.1668, 1962.
32. Keller, J.M. and Schaeffer, N.M.: Electr. Engng., Vol.79, No.12, p.1049, 1960.
33. - Pravda, TASS Report, May 17, 1963.